ACS Biomaterials SCIENCE & ENGINEERING

Article

pubs.acs.org/journal/abseba

Rapid Enhancement of Cellular Spheroid Assembly by Acoustically Driven Microcentrifugation

Layla Alhasan,[†] Aisha Qi,[‡] Aswan Al-Abboodi,[§] Amgad Rezk,[‡] Peggy P.Y. Chan,[‡,∥] Ciprian Iliescu,[⊥] and Leslie Y. Yeo*[,‡]

[†]Biotechnology & Biological Sciences, School of Applied Science, RMIT University, Melbourne, Victoria 3000, Australia

[‡]Micro/Nanophysics Research Laboratory, RMIT University, Melbourne, Victoria 3000, Australia

[§]Department of Chemical Engineering, Monash University, Clayton, Victoria 3800, Australia

[∥]Department of Biomedical Engineering, Swinburne University of Technology, Hawthorn, Victoria 3122, Australia

[⊥]Institute of Bioengineering and Nanotechnology, A*STAR, Singapore 138669, Singapore

Supporting Information

ABSTRACT: Intense acoustically driven microcentrifugation flows are employed to enhance the assembly of cellular spheroids in the microwell of a tissue culture well plate. This ability to interface microfluidics with commonly used tissue culture plasticware is a significant advantage as it can potentially be parallelized for high throughput operation and allows existing analytical equipment designed to fit current laboratory formats to be retained. The microcentrifugation flow, induced in the microwell coated with a low adhesive hydrogel, is shown to rapidly enhance the concentration of cells into tight aggregates within a minute—considerably faster than the conventional hanging drop and liquid overlay methods, which typically require days—while maintaining their viability. The proposed method also affords better control of the compaction force and hence the spheroid dimension simply by tuning the input power, which is a significant improvement over other microfluidic methods that require the fabrication of different geometries and microstructures to generate spheroids of different sizes. The spheroids produced are observed to exhibit the concentric heterogeneous cell populations and tight cell−cell interfaces typical of in vivo tumors, and are potentially useful in a broad spectrum of cancer biology and drug screening studies.

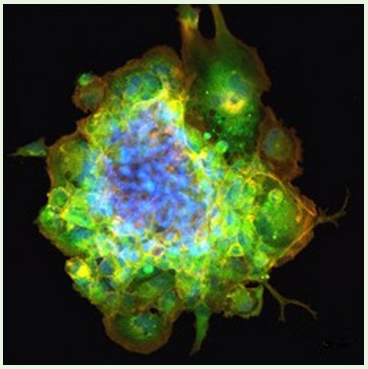

KEYWORDS: *microcentrifugation, spheroid, surface acoustic wave, hydrogel, cells*

1. INTRODUCTION

Cellular spheroids, comprising three-dimensional spherical cell aggregates displaying cell−cell and cell−matrix interactions, more closely mimic in vivo avascular tumor structure and functionality than conventional monolayer cultures in which intercellular contact is often lost.[1] They can therefore potentially be of fundamental importance to studies in cancer biology, metastasis and invasion, in addition to therapeutic screening.[2] Cellular spheroids have also been shown to play a role in improving the differentiation efficiency of mesenchymal stem cells.[3]

Various techniques have been used to produce these spheroids, all of which involve first the formation of loose cell aggregates, followed by their compaction into a tight spheroidal cluster;[1b] the different approaches vary primarily in the way the cells are driven to aggregate, and the method by which intercellular adhesion is promoted by preventing cell adhesion to the surface of a tissue culture dish.[4] The most widely used spheroidal culture technique to date is the hanging drop method[5] in which cell suspensions are first dispensed onto the lid of a Petri dish followed by inversion of the lid to form a hanging drop, each of which leads to the formation of a single cell aggregate. This method, however, requires careful balance between capillary and gravitational forces, is not practically amenable to medium exchange,[6] and is difficult to translate to large-scale production because the maximum permissible drop size is limited to 50 μL.[7] There have been recent attempts to address, for example, difficulties with medium exchange,[8] and a number of new commercial systems, such as the InSphero GravityPLUS and Sigma HDP 1096 Perfecta3D, allow hanging drops to form in well plates without the need for inversion, although these systems are generally significant in terms of their cost. Other systems, for example, the AggreWell by Stem Cell Technologies, involve centrifuging the entire well plate, therefore prohibiting individual addressability (because each well experiences the same centrifugation conditions). Moreover, the cell pellets that result tends to be pyramidal in shape with a large number of cells in poor contact with each other,[9] and, as such, the method necessitates at least a day of incubation to form the spheroid. In addition to its high cost, the Aggrewell plate also requires an additional step after the one-day period to filter out nonattached single cells prior to further

Received: March 12, 2016
Accepted: May 8, 2016
Published: May 9, 2016

Downloaded via RMIT UNIV on May 18, 2021 at 01:10:32 (UTC).
See https://pubs.acs.org/sharingguidelines for options on how to legitimately share published articles.

© 2016 American Chemical Society

DOI: 10.1021/acsbiomaterials.6b00144
ACS Biomater. Sci. Eng. 2016, 2, 1013−1022

incubation on the low attachment surface. Rotational bioreactors such as spinner flasks, on the other hand, have been employed for large-scale spheroid production and allow for medium exchange and cell sampling, although costly specialized culture equipment is required and the large shear stresses exerted lead to a tendency to fragment cells.[4]

Liquid overlay methods, in contrast, involve culturing a cell suspension over a three-day period on a weakly adhesive surface such as a thin agarose layer, agar gel or temperature-responsive methylcellulose coating atop a tissue culture dish.[10] Although simple, inexpensive, and amenable to scale-up, cell aggregation occurs quite serendipitously in these methods and thus the spheroids that are produced suffer from a fairly large variation in spheroidal quality.[1b,11] Further, agar performs poorly as a nonadhesive substrate.[10a] Additionally, agarose preparation requires the reagent to be autoclaved for dissolution and sterilization, followed by a long cooling period for the sol-gel transition. Temperature-responsive methylcellulose hydrogels, on the other hand, make medium exchange difficult because of their high viscosity and stringent temperature requirements.[10b] Other methods include suspension cultures in antiadhesive bacterial grade dishes to inhibit the attachment of adherent cells,[12] although it can be difficult to control the size and uniformity of the cell aggregates that are formed with these methods.[13]

More recently, various microfluidic strategies have been proposed for on-chip spheroid culture. These include microarray devices that immobilize cells on selectively adhesive patterned structures,[14] cell trapping barriers,[15] or nonadhesive microwells;[16] bubble and droplet-based methods in which the cells are encapsulated within bubble[2b] or gelated capsules;[17] cell trapping in microwells by ultrasonic actuation;[18] and microwells in which rotational flow of a cell suspension is induced.[19] Microarray methods possess the advantage of large-scale production of uniformly sized cell aggregates, although the aggregate size tends to be limited by the dimensions and the geometry of the patterns. Large numbers of cells also need to be seeded as any cells that are not immobilized tend to be washed away and lost.[15c] Bulk ultrasonic actuation, on the other hand, typically requires large transducers and custom-made microwells that facilitate the transmission of sound energy into the wells, and the necessity for relative high power is associated with considerable heating as well as long stabilization times (typically 15 min), which can be detrimental to the cells.[18] Bubble and droplet methods possess similar limitations as the aggregate sizes are dependent on that of the capsule, which, in turn, is restricted by the surface properties and dimensions of the microfluidic system. In addition, bubble methods suffer from low cell capture efficiencies. The rotational flow device, on the other hand, allows cell aggregates of different sizes to be produced from microwells of a single dimension, therefore circumventing the need to fabricate different devices to obtain aggregate size variation. However, the requirement of a filtration system to prevent cell clots from entering the device not only reduces the efficiency of the method due to loss of a large number of cells but also introduces further complexity embodied by the necessity for an additional channel shredder to break up large cell clots by shear.[19a] In addition, the closed microfluidic device restricts practical sampling and collection of cell aggregates, for example, for plating the cell aggregates to stimulate cell differentiation.[20]

Whichever approach is chosen, the low take-up of microfluidic technology at the bench has primarily been due to the inertia of practitioners such as laboratory technicians in adopting new and sophisticated technology, preferring instead to continue using familiar equipment and protocols even if these are inefficient and cost ineffective.[21] Another reason for their preference for existing laboratory formats in lieu of new technology can also be attributed to the existing compatibility of these methods to a vast array of ancillary laboratory technology, e.g., microscope stages, microplate readers, etc., that are already available without needing to invest in costly new equipment to accommodate the new format.

We therefore propose to interface a novel surface acoustic wave (SAW) microcentrifugation tool for rapid spheroid generation with a laboratory format that practitioners are already intimately familiar with and which has already been customized to fit a vast array of existing ancillary equipment for laboratory analysis, with the aim of exploiting the advantage of process improvement through new technology while allowing the user the benefit of retaining an existing format that they are accustomed to: the tissue culture microplate (Figure 1).

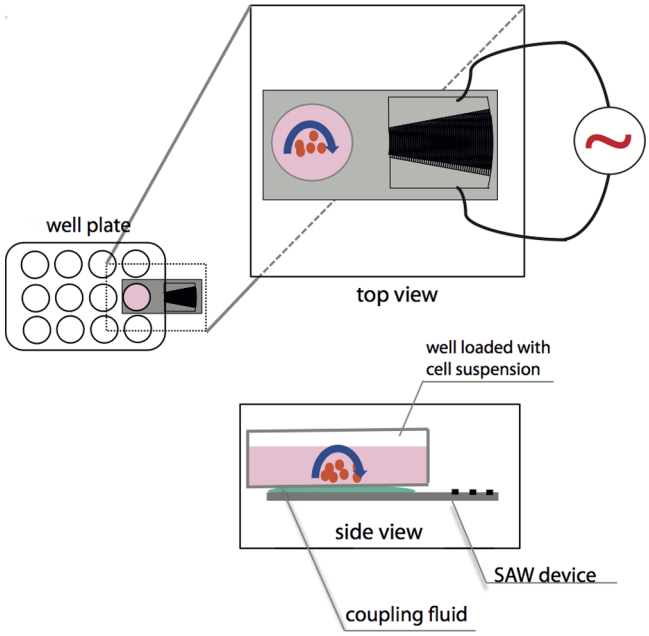

Figure 1. Schematic depiction of the setup used (not to scale) for rapid spheroid generation in a microwell on a well plate. The SAW device is interfaced from beneath using a fluid coupling layer. Representative images of the SAW device and the setup used are shown in Figure S1.

Microcentrifugation driven by SAWs—nanometer amplitude electromechanical waves localized on a chip-scale piezoelectric substrate[22]—has already been demonstrated for a variety of purposes, including chaotic micromixing[23] and rapid particle concentration[24] and sorting,[25] as well as to drive the rotation of small disks on which microchannels for a wide range of microfluidic operations can be patterned—the so-called miniaturized lab-on-a-disc;[26] this is in addition to the vast array of other microfluidic manipulations enabled by the SAW.[27] Unlike high-shear rotational bioreactors or other bulk ultrasonic devices which typically operate below 1 MHz, the 10−100 MHz order frequency SAWs which operate at very low (<1 W) powers, given the efficiency of the device, have significantly less tendency to denature large biomolecules and cells as there is insufficient time between the field reversal at

DOI: 10.1021/acsbiomaterials.6b00144
ACS Biomater. Sci. Eng. 2016, 2, 1013−1022

these frequencies compared to the shear relaxation time of molecules or cells; furthermore, cavitation—a common cause of biomolecular or cellular damage in ultrasonic devices—is also suppressed at these high frequencies and low powers.[28] SAWs, for example, have been employed not only to trap and position cells but also to control interactions between them.[29] Additionally, it has been shown that the MHz order SAW does not have any noticeable effect on the proliferation and differentiation characteristics of the cells.[30]

The fast (1−10 s order) SAW-driven microcentrifugation together with the use of a quick gelling hydrogel (carboxylmethyl cellulose tyramine; CMC-TYR) coating facilitates rapid production of tumor spheroids with controllable and uniform dimensions using standard tissue culture plasticware, in addition to allowing easy access for medium exchange and sampling, thus constituting a promising platform for studies in cancer biology and drug screening. We demonstrate the platform using human mammary gland carcinoma (BT-474) cells and primary cells, in particular, rat mesenchymal stem cells (MSCs). The former was employed because BT-474 cell lines exhibit tumorigenic potential in vivo[31] and has the propensity to form spheroids whose properties are well documented,[32] thus constituting a good model cancer cell line. The latter was adopted not only because MSCs have been shown for spheroid formation in previous work,[33] but also because they are less prone and hence more difficult to form spheroids compared to cancer cells. Although SAWs have been previously coupled into superstrates on which sessile drops are manipulated,[34] the use of SAWs to drive microcentrifugation in a standard tissue culture well plate has yet to be demonstrated. Moreover, we will show that the technique not only allows rapid cell aggregation with small numbers of cells, but also facilitates control of the spheroid dimension simply by tuning the power input to the SAW, therefore removing the need, for example, for elaborate fabrication of different microstructures.

2. MATERIALS AND METHODS

We outline in this section the method employed for the generation and characterization of the spheroids. The materials used and other methods associated with the fabrication of the SAW devices, the synthesis of the hydrogel, the cultivation of the cells, and the examination of the F-Actin organization in the spheroids, are given in Section S1 in the Supporting Information, whereas details on the hydrogel characterization are given in Section S2.

S2.1. Spheroid Generation. A cell suspension was first prepared by suspending the BT-474 cells or primary cells comprising GIBCO rat MSCs with the desired cell density (2×10^3, 4×10^3, 5×10^3, or 6×10^3 cells/mL for the BT-474 cells and 500 cells per well for the MSCs) in cell culture medium, followed by the addition of 1% gelatin to the cell culture medium as an intercellular linker to assist cell aggregation. Here we demonstrate the feasibility of generating the spheroids using SAW microcentrifugation in both a 12-well plate and 96-well plate. Specifically, the microwells of the microplate were coated with a thin layer of CMC-TYR (167 μL/cm^2) that functioned as a low-adhesive coating and subsequently filled with 20 μL of cell suspension. Acoustic energy was then transmitted into the microwell to induce the microcentrifugation flow within it for the purpose of driving the cells to aggregate. This was carried out by placing the SAW device beneath the microwell, sandwiching a thin layer of fluid couplant consisting of KY Jelly (Chemist Warehouse, Virginia, QLD, Australia) in between. This technique for acoustic energy coupling from the SAW device into a superstrate layer was first demonstrated by Hodgson et al.,[34a] and later employed for a variety of acousto-microfluidic operations on superstrates.[34b,c] The microcentrifugation flow itself is generated by introducing asymmetry in the delivery of the acoustic wave with respect to the geometry of the drop or microwell,[35] achieved most easily here by simply offsetting the drop or microwell with respect to the elliptical single-phase unidirectional transducers (SPUDTs).

The SAW device, details for the fabrication of which are given in Section S1.2, was activated by supplying an oscillating electrical signal at the resonance frequency of 30 MHz to the SPUDT for 1 min using a multifunction synthesizer (Wave Factory WF1966 2CH, NF Corporation, Yokohama, Japan) and coaxial amplifier (Mini-Circuits ZHL-1−2W, RS Components Pty. Ltd., Sunshine West, VIC, Australia) to induce the microcentrifugation flow within the well in order to drive the cell aggregation. Once the cell aggregate was formed, 100 μL of medium was carefully added to the well; we note that the volume of medium that can be added depends on the dimensions of the well—greater volumes up to milliliters can typically be employed for wells with larger radial dimensions which allow more transmission of the acoustic energy from the device into the well as long as the aperture of the acoustic wave is not exceeded. The position of the SAW device beneath the well plate was then moved under other wells in order to repeat the same spheroid generation process as required, although multiple SAW devices, one under each well, are currently being developed to run multiple microcentrifugation processes in parallel for high throughput operation.

Spheroids were also produced using the liquid overlay method for comparison. In brief, a 20 μL cell suspension containing the intercellular linker was prepared in the same manner and with the same seeding density as those used for the SAW microcentrifugation. The cell suspension was transferred to microwells that were precoated with a thin layer of CMC-TYR (167 μL/cm^2) and topped up with 100 μL of medium. In both cases, the microwell plates were then transferred to a 5% CO_2 humidified incubator for further spheroid cultivation at 37 °C. Wells that were not subjected to the acoustic irradiation were used as controls.

S2.2. Characterization of the Spheroid Viability, Morphology, and Proliferation. Cell viability was evaluated using a LIVE/DEAD Cell Viability Assay (Life Technologies, Mulgrave, VIC, Australia) according to the manufacturer's protocol prior to which the cells were incubated for 2 h after the SAW irradiation. To investigate the cell distribution within the spheroid, we cultured the spheroids produced for 10 days and then collected by centrifuging at 300 rpm. The collected spheroids were subsequently fixed with 4% paraformaldehyde followed by rinsing in PBS, and finally subjected to Tissue Tek O.C.T. (Sakura Finetek Inc., Torrance, CA) embedding. Histochemical analysis was then performed on 5 μm sections of the spheroid. The sections were further stained by hematoxylin and eosin (H&E) using standard procedures.[36] The morphology of the H&E, calcein AM and propidium iodide (PI) stained spheroids were visualized using optical microscopy (CKX41, Olympus Pty. Ltd., Notting Hill, VIC, Australia) and laser scanning confocal microscopy (LSCM; Eclipse Ti Confocal Microscope, Nikon Instruments Inc., Melville, NY), respectively. The diameter and cross-sectional area as well as the perimeter of the spheroids were measured from different angles using ImageJ across multiple samples (National Institutes of Health, Bethesda, MD). The irregularity parameter IP, defined as the ratio of the diameter of the minimum circumscribed circle D to that of the maximum inscribed circle d (Figure S5), i.e., $IP \equiv D/d$,[37] was used as an indicator to evaluate the circularity of a spheroid; an IP with a value of 1 indicates a perfect circle, whereas a large IP value indicates that the spheroid exhibits irregular morphology. For the spheroid proliferation studies, the spheroids were cultured and subsequently monitored for a period of 10 days after being exposed to the SAW. The same viability and morphology characterization studies were employed as that detailed above. The spheroids were collected for trypsinization at different time points, and the number of cells proliferating within was determined by measuring the DNA content using the Quanti-iT PicoGreen dsDNA Assay (Life Technologies, Mulgrave, VIC, Australia).[38] For the control, cells were allowed to aggregate using the conventional liquid overlay method on a CMC-TYR coated well plate, and monitored in the same way.

DOI: 10.1021/acsbiomaterials.6b00144
ACS Biomater. Sci. Eng. 2016, 2, 1013−1022

3. RESULTS AND DISCUSSION

3.1. SAW Microcentrifugation Driven Cell Aggregation as a Precursor to Spheroid Formation. Representative images of the BT-474 spheroids generated using the SAW device compared to the control experiment in which the acoustic irradiation and hence the microcentrifugation flow was absent are shown in Figure S6. Also shown are the representative results when the hydrogel low-adhesive coating was absent. It can generally be seen for the uncoated microwell (top row images in Figure S6) that more cells were concentrated as a result of the microcentrifugation flow in the well due to the applied acoustic irradiation compared to the control experiment in which no external forces were applied and the cells simply sedimented under gravity.

We observe the yield of the SAW microcentrifugation method to be high, wherein 87.0 ± 4.2% of the seeded cells were found to aggregate into a single spheroid (Figure S7 in the Supporting Information). Moreover, we observed that all the cells recovered from the SAW microcentrifugation appeared to be viable. The relationship between the number of cells in the aggregate as a function of the input power is discussed below. Nevertheless, we note that despite the concentration arising from the SAW microcentrifugation flow, particularly for the case of the microwell (which remains qualitatively similar to that in a sessile drop[39]), a large number of cells remained in a spokelike pattern instead of being concentrated into a tight pallet at the center of the well. We believe this is due to standing waves that arise as a consequence of the reflection of sound waves from the walls of the well; in other words, the well forms an effective acoustic cavity. It is well-known that particles and cells with densities greater than the surrounding fluid are easily trapped at the nodes of standing waves where the acoustic radiation pressure is at its minimum.[40] In addition, the absence of a weakly adhesive coating meant that the cells tended to adhere to the bottom of the well.

It can, however, be seen from the bottom row images in Figure S6 that these difficulties in attempting to drive the cells into a tightly packed aggregate, which have a direct effect on the quality of the spheroids that can be formed, can be circumvented simply by coating the microwell with the hydrogel. In the presence of the coating, we observe the cells to be concentrated into a tight aggregate; it can also be clearly seen that a considerably larger aggregate cell density can be achieved when the cells are concentrated by the SAW-driven microcentrifugation flow. The disappearance of the spokelike cell patterns with the use of the hydrogel coating also suggests that the hydrogel plays a twofold role in not only preventing cell adhesion along surfaces but also in absorbing the sound wave and thus preventing its reflection and hence the generation of standing waves in the well.

The effect of the applied SAW power, which has a direct consequence on the velocity of the induced microcentrifugation flow in the well, is shown in Figure S8. The viability of the cells is also indicated in the figure given that the cells were stained with calcein AM which is not only permeable through the cell membrane but also fluoresces when internalized and hydrolyzed by live cells; further, no PI stained cells (dead cells) were observed. Consistent with previous findings on the effect of SAW irradiation on the viability of cells,[28] we observe the majority, if not all, of the cells to remain intact and to fluoresce with the green calcein AM stain, indicating the retention of their viability across the range of applied powers (0.5−1.53 W) employed.

The morphology of the cell aggregates and hence the subsequent spheroid formation, however, depends intimately on the applied power as well as the cell seeding densities (2×10^3 to 6×10^3 cells/ml) employed. In order to obtain quantitative morphometric characterization, we examine both the spheroid cross-sectional area and irregularity parameter *IP* as a function of these system parameters. The former is a measure of the compactness of the spheroid formed, whereas the latter is a measure of the circularity of the spheroid (*IP* values close to 1 correspond to more circular spheroids). Figure 2 shows that for a fixed applied power, the cross-sectional area

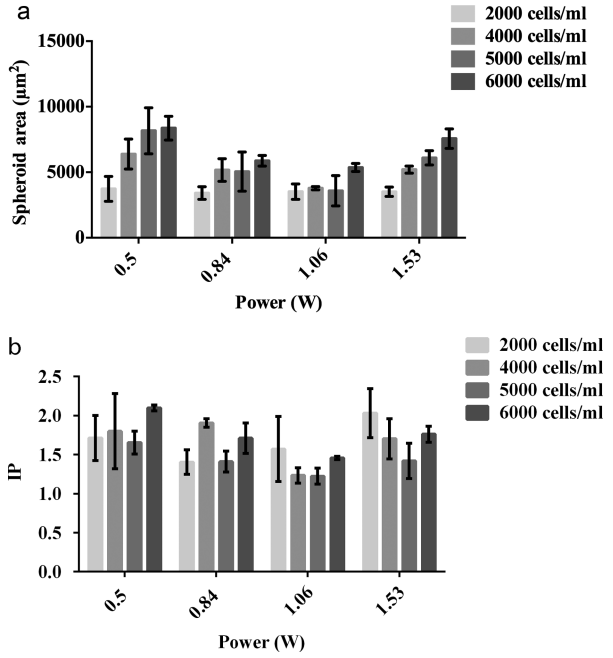

Figure 2. Effect of the applied SAW power on (a) the cross-sectional area, and, (b) the irregularity parameter *IP* of BT-474 spheroids. The spheroids were obtained 2 h after the SAW was applied to drive the microcentrifugation flow. The error bars represent the standard deviation (n = 3).

of the BT-474 spheroids increased with increasing seeding density, for the simple reason that more cells aggregate into the spheroid thus leading to a larger intrinsic volume; at low cell seeding densities, the correlation between power is less obvious, because a critical cell number has not been reached to produce a measurable difference in the *IP* and spheroid cross-sectional area.

Beyond this critical seeding density, however, we find that the smallest spheroid cross-sectional area, i.e., the most compact and circular spheroids were obtained at intermediate powers around 1 W, consistent with previous findings on SAW microcentrifugation driven particle concentration which found that the tendency for particles to concentrate increased with the applied power and hence the intensity of the microcentrifugation flow until a point beyond which the increasingly rapid convective flow overcame the diffusion-driven particle concentration dynamics thereby leading to redispersion of the particles.[35] The existence of an optimum at intermediate applied powers is also true for *IP* values close to 1 given that excessive convective dispersion at high microcentrifugation

DOI: 10.1021/acsbiomaterials.6b00144
ACS Biomater. Sci. Eng. 2016, 2, 1013−1022

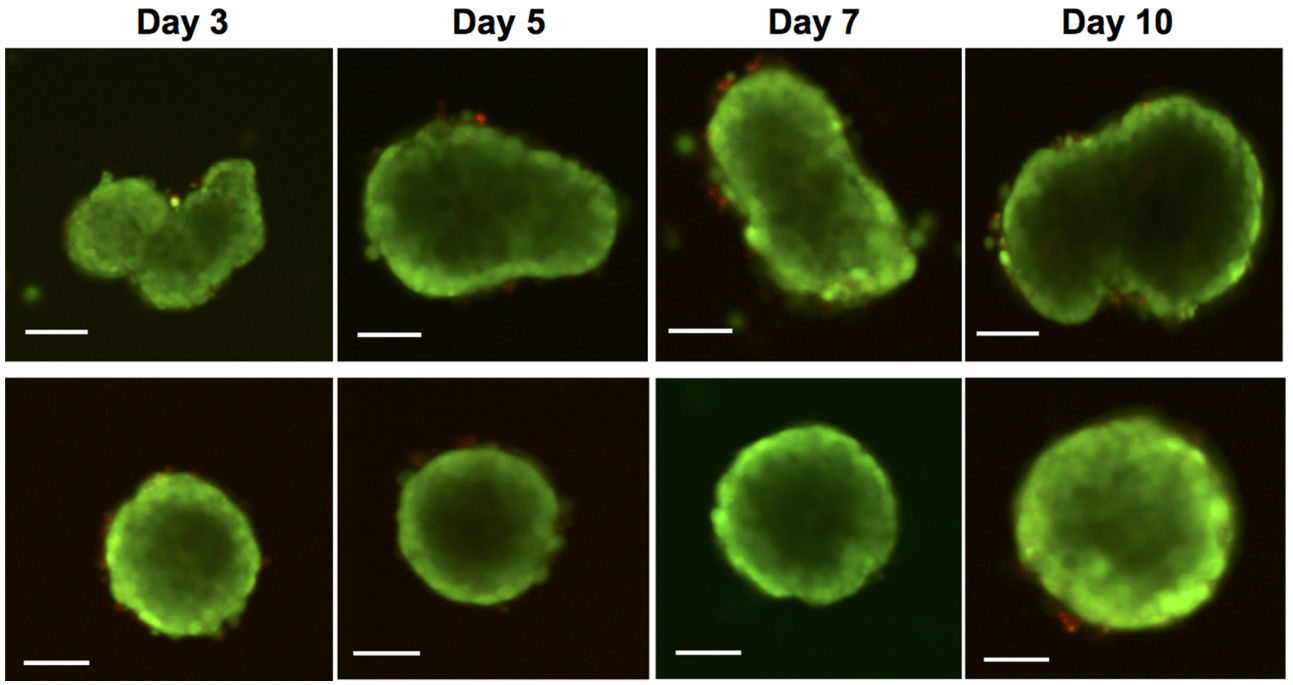

Figure 3. Representative confocal microscopy images showing the viability of BT-474 spheroids cultured using both the liquid overlay (LO, top panel) and SAW microcentrifugation (SAW, bottom panel) methods over a period of 10 days. In both cases, the spheroids were prepared from a seeding density of 5×10^3 cells/mL. In the latter case, the input power to the SAW device is 1.06 W. The spheroids were stained using the live/dead cell viability assay. Live cells, which appear green, are stained by calcein AM; dead cells, which appear red, are stained by propidium iodide (identical figures showing separate red and green channels are provided in Figure S11). The necrotic core of the cells can thus be seen given the absence of coloration in the center of the spheroids. Scale bars represent 100 μm lengths.

velocities leads to increasingly chaotic flow[23] that promotes increasing irregularity in the cell aggregates. Further, we note that the optimum shifts slightly to higher powers for larger cell seeding densities given that greater microcentrifugation velocity thresholds are necessary to concentrate and also to disperse larger numbers of cells given the increase in the intrinsic viscosity with higher cell concentrations.[41]

In contrast to directly centrifuging the entire well plate atop a rotary shaker, which tends to lead to the formation of pyramidal shaped cell pellets in which a large number of cells are in poor contact with each other, the ability of the SAW microcentrifugation to drive cells rapidly to the center of the well at an optimum applied power to allow some degree of control over the uniformity of the spheroid formation for different cell densities is a significant advantage given the importance of the uniformity of spheroids, especially for many cell-based assays.[15a] Nonuniform spheroids commonly lead to nonuniformities in the exposure and diffusion of reagents to the cells, thus resulting in large variation in the observed cell behavior. In addition, image analysis in these studies is also complicated by irregularity in the spheroid morphology.[42] This is in contrast to other microfluidic techniques such as the microarray and microcapsule based approaches, which can only yield spheroids of a fixed size range for a given system geometry, therefore requiring expensive and laborious steps in tailoring different photomasks for the fabrication of different microstructures for each cell seeding density and desired size range.

3.2. Spheroid Proliferation. The representative confocal microscopy images in Figure 3 shows that the size of the BT-474 spheroids generated by both the SAW microcentrifugation method as well as the liquid overlay method (control) increased over time, indicating the proliferation of cells within; the viability of cells inside the spheroids again being evaluated using live/dead cell viability staining in which live cells were stained by calcein AM and appear in green whereas dead cells on the other hand were stained by PI and appear in red. Notwithstanding the limitation of confocal microscopy imaging to a 50 μm depth, thus restricting the ability to observe the core of large spheroids—which could explain the absence of coloration in the center of the spheroids in Figure 3, a likely possibility is that most of the cells on the periphery of the spheroids remain viable, thus forming a shell around a necrotic core that is evidenced by an absence of coloration in the center of the spheroids. Although PI can penetrate through the leaky membrane of dead cells to stain the cell nuclei, it is nevertheless impermeable to live cells in contrast to calcein AM.[43] As such, PI therefore does not infiltrate the outer viable cell layer to reach the cells at the center of the spheroids. Such necrotic cores are common in tumor spheroids, especially in older and larger spheroids, where the cells in the center of the tumor spheroid are deprived of oxygen and nutrients due to diffusion limitations.[2a,44] It was observed that the ratio of the size of the necrotic core to that of the whole spheroid increased with time (Figure S9), because of the increasing severity of these nutrient deprivation conditions as the spheroid grows. As in vivo tumors are known to develop necrotic cores as their sizes increase,[45] spheroids with necrotic cores are therefore employed as an in vitro mimic of tumor development patterns.[46] Parenthetically, we also note that a small number of dead cells can be seen on the spheroid surface in Figure 3 (corresponding to the non-100% yield in Figure S7), which are likely to be free-floating cells present in the cell culture medium that were not completely washed off by the rinse step during staining, despite

DOI: 10.1021/acsbiomaterials.6b00144
ACS Biomater. Sci. Eng. 2016, 2, 1013−1022

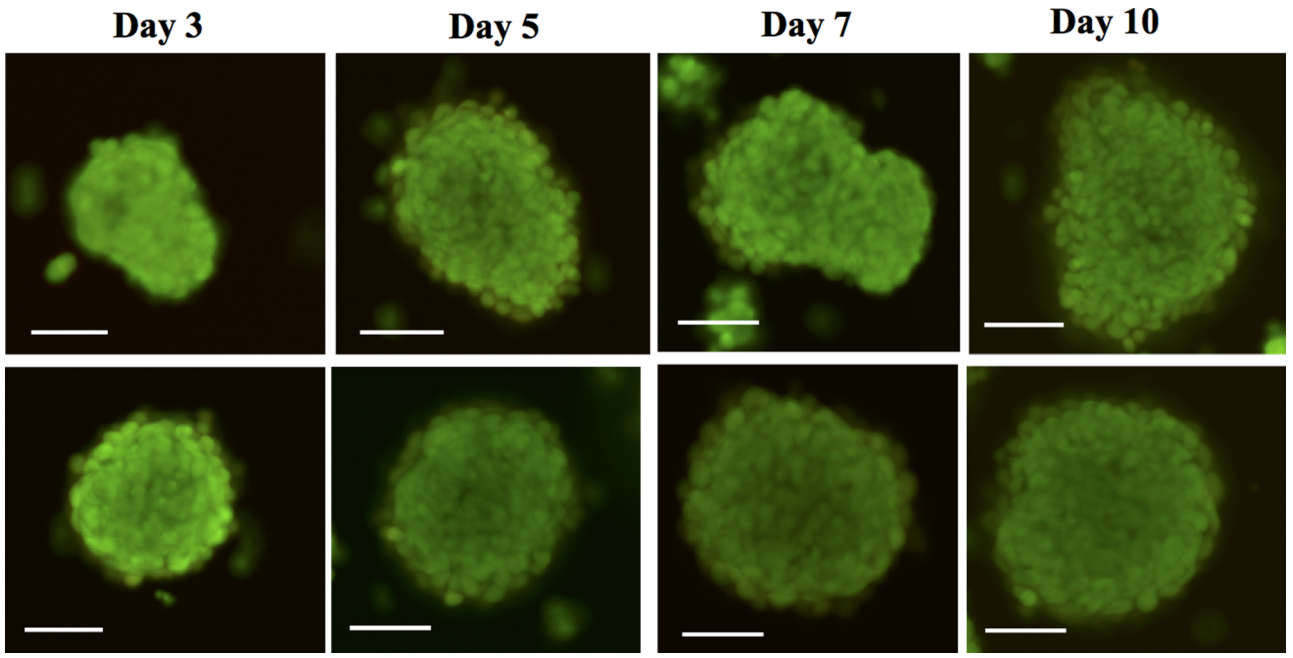

Figure 4. Representative confocal microscopy images showing the viability of MSC spheroids cultured using both the liquid overlay (LO, top panel) and SAW microcentrifugation (SAW, bottom panel) methods over a period of 10 days. In both cases, the spheroids were prepared from a seeding density of 500 cells/well. In the latter case, the input power to the SAW device is 1.06 W. The spheroids were stained using the live/dead cell viability assay. Live cells, which appear green, are stained by calcein AM; dead cells, which appear red, are stained by propidium iodide (identical figures showing separate red and green channels are provided in Figure S11). Scale bars represent 100 μm lengths.

this being carried out gently to avoid distortion of the spheroids.

Similar to that observed for BT-474 spheroids, Figure 4 shows that the size of the MSC spheroids generated by both the SAW microcentrifugation method as well as the liquid overlay method increased with time, indicating the propensity of the cells that constitute the spheroid to continue proliferating. This is confirmed by the live/dead cell viability assay, which demonstrated that the majority of the MSCs within the spheroids remained viable (which appear green). These results further verify that the SAW microcentrifugation technique does not pose adverse effects on the cells regardless of their type, especially because MSCs are considerably more fragile than those from cancer cell lines. Additionally, these results also further validate the feasibility of the SAW microcentrifugation technique for spheroid cultivation in a primary cell line less prone to spheroid formation.

The proliferation of the cells forming the spheroids was assessed by determining their DNA content, given that DNA is a cellular component that accurately reflects the cell number. Figure 5 shows that the number of BT-474 cells in the spheroids cultured using both the SAW microcentrifugation method (p = 0.01, n = 3) and liquid overlay method (p < 0.001) increased gradually over a 7-day period indicating that the cells proliferate within the spheroids. This is confirmed by the quantitative data in Figure 6 showing the mean diameter for the BT-474 spheroids produced from the SAW microcentrifugation method (p < 0.0001, n = 5) increasing over time. Meanwhile, the spheroids produced using the liquid overlay method exhibit relatively large variation in diameter within the same sample group due to their irregular shapes. We note in general that the spheroid size is smaller and that a lower irregularity parameter of the spheroid closer to a value of 1 was obtained using the SAW microcentrifugation method compared

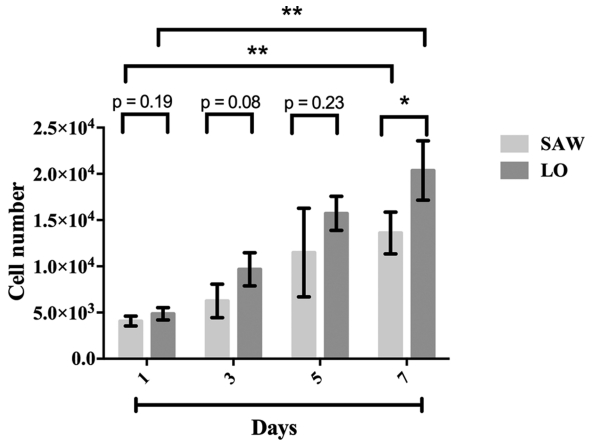

Figure 5. Gradual increase in the proliferation of BT-474 cells in spheroids cultured using both the liquid overlay (LO) and SAW microcentrifugation methods (at an applied power of 1.06 W) over a period of 7 days. In both cases, the spheroids were prepared from a seeding density of 5 × 10^3 cells/mL. The error bars represent the standard deviation (n = 3).

to spheroids obtained with the liquid overlay method. This is more likely related to the shape and compactness of the spheroids rather than to their viability given the absence of adverse effects due to the SAW microcentrifugation on the cells, as indicated by the results from the live/dead cell viability (Figure S8) and proliferation (Figure 5) assays. In any case, this result alludes to the possibility of synthesizing more uniform and compact spheroids using the SAW microcentrifugation method, and allowing them to be potentially more useful for cell-based assays.

Moreover, the BT-474 spheroids that were produced via both methods appeared to exhibit heterogeneous cell

DOI: 10.1021/acsbiomaterials.6b00144
ACS Biomater. Sci. Eng. 2016, 2, 1013−1022

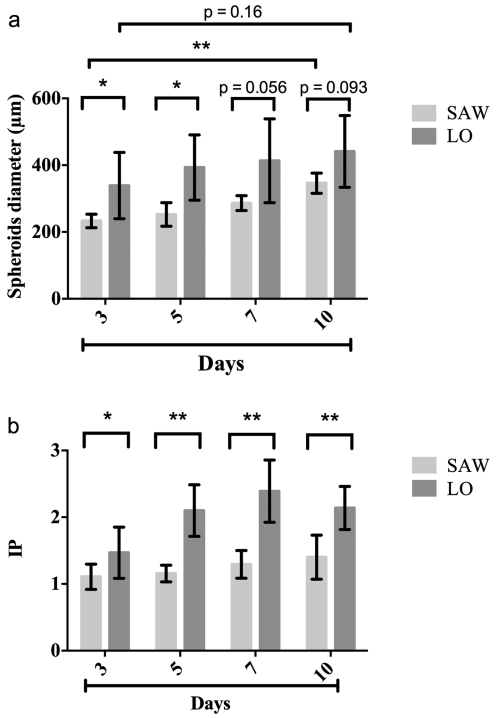

Figure 6. (a) Diameter and (b) irregularity parameter *IP* of BT-474 spheroids obtained using both the conventional liquid overlay (LO) and SAW microcentrifugation (SAW) methods with a seeding density of 5×10^3 cells/ml. In the latter case, the input power to the SAW device is 1.06 W. From (a), it can be seen that the mean diameter of the spheroids produced by SAW microcentrifugation increased over time ($p < 0.0001$). The single and double asterisks indicate p values below 0.05 and 0.01, respectively. The error bars represent the standard deviation ($n = 5$).

subpopulations that contained viable cells at their periphery and nonviable cells in their necrotic core. Figure S10 is a representative histological section of a spheroid produced with the SAW microcentrifugation method showing the distribution of cells within; nuclei appear in violet given the H&E staining. It can be observed that a large number of cells are tightly packed within the spheroid, typical of tumor morphology.[2a] It is this tight packing that limits nutrient and oxygen diffusion into the spheroid interior, thus resulting in the necrotic cores observed in Figure 3. Indeed, such concentric heterogeneous cell populations of spheroids mimic the avascular stage of tumors in vivo,[47] making the in vitro spheroid model a useful tool for cancer biology studies.

3.3. F-Actin Organization. The cytoskeleton organization and focal adhesion contact of the spheroids that were generated using the SAW microcentrifugation method compared to that of monolayer cells are shown by the representative images in Figure 7. Actin filaments in the cytoskeleton of the spheroids were stained by TRITC-conjugated phalloidin and shown in red, while the focal adhesion marker vinculin was stained by fluorescently labeled antivinculin monoclonal antibody and shown in green. It can be seen that the monolayer cells exhibited the usual spindle morphology and displayed more well-spread actin filaments and typical cell−substrate adhesion. In contrast, the organization of the actin filaments is more irregular in the spheroids whereas the vinculin appears co-localized especially at the center of the spheroid; such co-localization was first observed in the SAW generated spheroids after 7 days of cultivation and increased progressively over 20 days. Compared to monolayer cells, the mean fluorescence intensity (MFI) of vinculin observed in the LSCM images of the SAW spheroids was found to be significantly higher ($p < 0.0001$, $n = 20$), as shown in Figure 8, again indicating greater co-localization of vinculin in the spheroids. This is simply

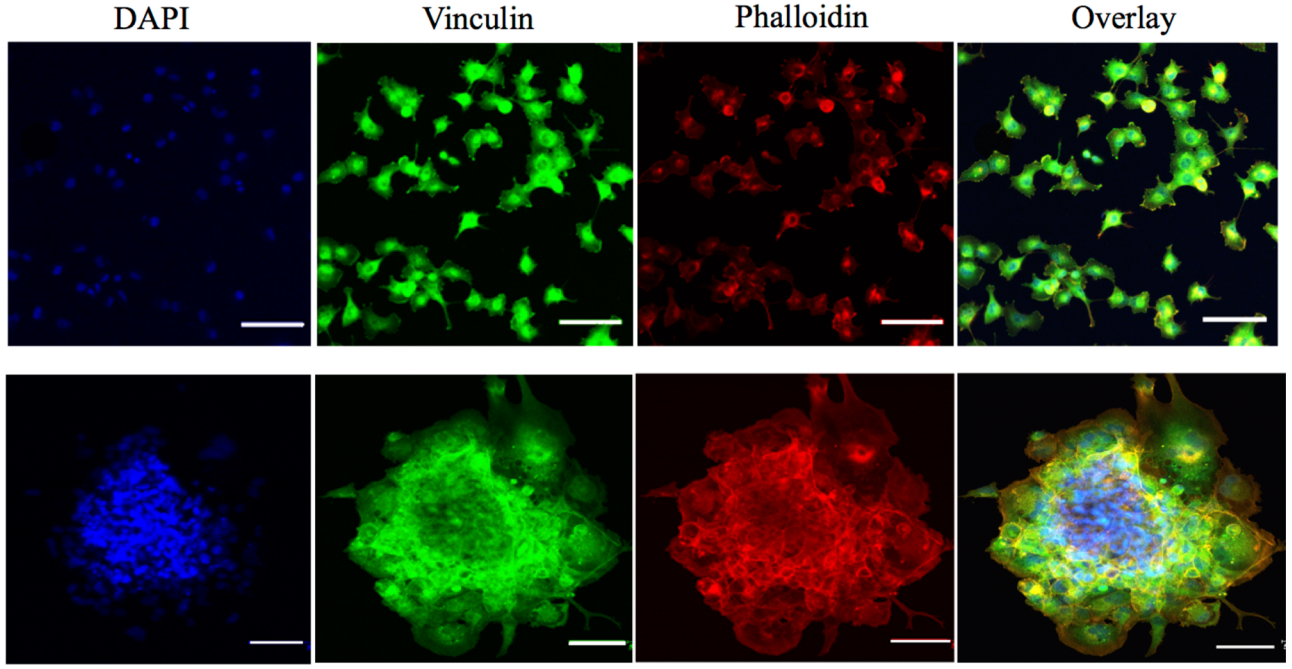

Figure 7. Representative confocal microscopy images revealing the focal adhesion points and nuclei of monolayer BT-474 cells (top panel, control) and that of a 20-day old BT-474 spheroid generated using the SAW microcentrifugation device at an applied power of 1.06 W (bottom panel). Nuclei were stained by DAPI and displayed in blue, focal contacts were stained by antivinculin antibody and displayed in green, whereas F-actin was stained by TRITC-conjugated phalloidin and displayed in red. Images were overlaid in the last column. The scale bars represent 100 μm lengths.

DOI: 10.1021/acsbiomaterials.6b00144
ACS Biomater. Sci. Eng. 2016, 2, 1013−1022

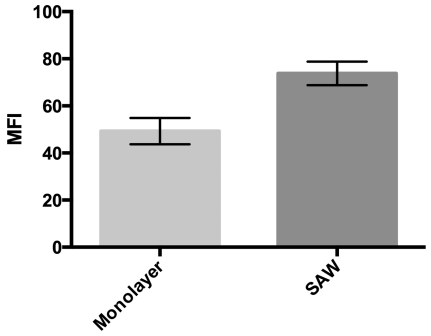

Figure 8. Mean fluorescence intensity (MFI) of vinculin expressed in monolayer BT-474 cells (control) and 20-day old BT-474 spheroids generated using the SAW microcentrifugation device at an applied power of 1.06 W. We observe the mean fluorescence intensity in the former is significantly lower than that in the latter ($p < 0.0001$). The error bars represent the standard deviation ($n = 20$).

because more cells are packed in the 3D structure compared to that in the monolayer culture. Together, these reveal the possibility for the production of 3D spheroid structures with the SAW microcentrifugation method.

4. CONCLUSION

In summary, we demonstrate the feasibility of interfacing a SAW microfluidic device with a superstrate, which could constitute a tissue culture dish or a microarray well plate, for the controlled generation of uniform cellular spheroids. This has considerable advantages over other microfluidic devices for spheroid production given that existing laboratory formats already well familiar with biologists and laboratory technicians and for which ancillary equipment such as microscopes and plate readers have been designed to fit are retained without requiring further investment into new analytical equipment. Further, the chip-scale dimensions of the SAW device, as well as its low-cost by exploiting the economies-of-scale associated with large volume nanofabrication, facilitate scale-out (i.e., numbering up) for high throughput operation: while we have demonstrated the use of a SAW device to enhance spheroid production in a single microwell on a standard tissue culture microplate, the use of multiple SAW devices in parallel, one under each well, for example, can easily be envisaged. This is relatively straightforward and allows the possibility for individual addressability of each well, although necessitating the development of a circuit controller.

The acoustic irradiation is coupled into the microwell through a fluid couplant layer sandwiched in between. Through symmetry breaking of the sound waves in the liquid, an intense microcentrifugation flow can be induced in the microwell, which drives the concentration of the cells into a tight aggregate. This is aided by the use of a low-adhesive hydrogel coating on the microwell walls, which prevents cell adhesion to the wall and suppresses standing sound waves which trap cells at nodal positions away from the center. We show that compact and circular spheroids can be generated, whose size can be controlled by tuning the input power of the SAW: the most compact and uniform (in terms of circularity) spheroids were obtained at intermediate powers since a trade-off exists between the increasing concentration and aggregation of cells with more intense microcentrifugation flow as the power is increased and the increasingly dispersive nature of the intense chaotic flow at high powers beyond a threshold value. This optimum power is observed to depend on the cell seeding density. In any case, the ability for spheroidal size control simply through the input power represents a distinct improvement because it circumvents the need for the fabrication of multiple devices with various geometric designs. Moreover, only a small number of cells are needed for the seeding which is important for applications in which cells are scarce, for example, in the generation of embryoid bodies from human stem cells or human induced pluripotent stem cells. Furthermore, the cell concentration process is rapid, requiring only a minute, compared to other conventional methods such as the liquid overlay methods which require at least a day; the fast gelation rate of the CMC-TYR hydrogel also considerably reduces the preparation time for coating the tissue culture surface. Compared to the conventional hanging drop method, the SAW microcentrifugation method has the advantage of being able to handle larger fluid volumes through parallelization by scaling out the operation. Further, the resulting spheroids exhibited the concentric heterogeneous cell population arrangement and tight cell-to-cell interfaces typically observed in solid tumors in vivo, thus demonstrating the potential usefulness of the platform for improving cancer biology and drug screening investigations.

■ ASSOCIATED CONTENT

Supporting Information

The Supporting Information is available free of charge on the ACS Publications website at DOI: 10.1021/acsbiomaterials.6b00144.

Supporting Information comprising more detailed description of the methods as well as additional results (PDF)

■ AUTHOR INFORMATION

Corresponding Author

*E-mail: leslie.yeo@rmit.edu.au.

Notes

The authors declare no competing financial interest.

■ ACKNOWLEDGMENTS

Funding for this work was partly provided through Australian Research Council Discovery Grants DP120102570 and DP140100805. The authors also thank Dr. Anna Walduck for her assistance with cryostat cutting. L.A. is grateful for a PhD scholarship from the Ministry of Higher Education and Scientific Research, Iraq. L.Y.Y. gratefully acknowledges support through a Future Fellowship from the Australian Research Council under Grant FT130100672.

■ REFERENCES

(1) (a) Korff, T.; Augustin, H. G. Integration of Endothelial Cells in Multicellular Spheroids Prevents Apoptosis and Induces Differentiation. *J. Cell Biol.* **1998**, *143* (5), 1341−1352. (b) Lin, R.-Z.; Chang, H.-Y. Recent advances in three-dimensional multicellular spheroid culture for biomedical research. *Biotechnol. J.* **2008**, *3* (9−10), 1172−1184.

(2) (a) Khaitan, D.; Chandna, S.; Arya, M. B.; Dwarakanath, B. S. Establishment and characterization of multicellular spheroids from a human glioma cell line; Implications for tumor therapy. *J. Transl. Med.* **2006**, *4* (1), 12. (b) Agastin, S.; Giang, U.-B. T.; Geng, Y.; DeLouise, L. A.; King, M. R. Continuously perfused microbubble array for 3D tumor spheroid model. *Biomicrofluidics* **2011**, *5* (2), 024110.

DOI: 10.1021/acsbiomaterials.6b00144
ACS Biomater. Sci. Eng. 2016, 2, 1013−1022

(c) Mueller-Klieser, W. Multicellular spheroids. *J. Cancer Res. Clin. Oncol.* **1987**, *113* (2), 101−122.
(3) (a) Bosnakovski, D.; Mizuno, M.; Kim, G.; Takagi, S.; Okumura, M.; Fujinaga, T. Chondrogenic differentiation of bovine bone marrow mesenchymal stem cells (MSCs) in different hydrogels: Influence of collagen type II extracellular matrix on MSC chondrogenesis. *Biotechnol. Bioeng.* **2006**, *93* (6), 1152−1163. (b) Frith, J. E.; Thomson, B.; Genever, P. G. Dynamic Three-Dimensional Culture Methods Enhance Mesenchymal Stem Cell Properties and Increase Therapeutic Potential. *Tissue Eng., Part C* **2010**, *16* (4), 735−749.
(4) Sarvi, F.; Arbatan, T.; Chan, P. P. Y.; Shen, W. A novel technique for the formation of embryoid bodies inside liquid marbles. *RSC Adv.* **2013**, *3* (34), 14501−14508.
(5) Kelm, J. M.; Timmins, N. E.; Brown, C. J.; Fussenegger, M.; Nielsen, L. K. Method for generation of homogeneous multicellular tumor spheroids applicable to a wide variety of cell types. *Biotechnol. Bioeng.* **2003**, *83* (2), 173−180.
(6) Kurosawa, H. Methods for inducing embryoid body formation: in vitro differentiation system of embryonic stem cells. *J. Biosci. Bioeng.* **2007**, *103* (5), 389−398.
(7) Arbatan, T.; Al-Abboodi, A.; Sarvi, F.; Chan, P. P. Y.; Shen, W. Tumor Inside a Pearl Drop. *Adv. Healthcare Mater.* **2012**, *1* (4), 467−469.
(8) Frey, O.; Misun, P. M.; Fluri, D. A.; Hengstler, J. G.; Hierlemann, A. Reconfigurable microfluidic hanging drop network for multi-tissue interaction and analysis. *Nat. Commun.* **2014**, *5*, 4250.
(9) (a) Baraniak, P.; McDevitt, T. Scaffold-free culture of mesenchymal stem cell spheroidsin suspension preserves multilineage potential. *Cell Tissue Res.* **2012**, *347*, 701−711. (b) Wrzesinski, K.; Fey, S. After trypsinisation, 3D spheroids of C3A hepatocytesneed 18 days to re-establish similar levels of keyphysiological functions to those seen in the liver. *Toxicol. Res.* **2013**, *2*, 123−135. (c) Razian, G.; Yu, Y.; Ungrin, M. Production of Large Numbers of Size-controlled Tumor Spheroids Using Microwell Plates. *J. Visualized Exp.* **2013**, *81*, e50665.
(10) (a) Carlsson, J.; Yuhas, J. M., Liquid-Overlay Culture of Cellular Spheroids. In *Spheroids in Cancer Research*, Acker, H., Carlsson, J., Durand, R., Sutherland, R., Eds.; Springer: Berlin, 1984; Vol. *95*, pp 1−23. (b) Yang, M.-J.; Chen, C.-H.; Lin, P.-J.; Huang, C.-H.; Chen, W.; Sung, H.-W. Novel Method of Forming Human Embryoid Bodies in a Polystyrene Dish Surface-Coated with a Temperature-Responsive Methylcellulose Hydrogel. *Biomacromolecules* **2007**, *8* (9), 2746−2752. (c) Walser, R.; Metzger, W.; Görg, A.; Pohlemann, T.; Menger, M.; Laschke, M. Generation of co-culture spheroids as vascularisation units for bone tissue engineering. *Eur. Cell Mater.* **2013**, *26*, 222−233. (d) Metzger, W.; Sossong, D.; Bächle, A.; Pütz, N.; Wennemuth, G.; Pohlemann, T.; Oberringer, M. The liquid overlay technique is the key to formation of co-culture spheroids consisting of primary osteoblasts, fibroblasts and endothelial cells. *Cytotherapy* **2011**, *13*, 1000−1012.
(11) (a) Takezawa, T.; Yamazaki, M.; Mori, Y.; Yonaha, T.; Yoshizato, K. Morphological and immuno-cytochemical characterization of a hetero-spheroid composed of fibroblasts and hepatocytes. *J. Cell Sci.* **1992**, *101* (3), 495−501. (b) Fennema, E.; Rivron, N.; Rouwkema, J.; van Blitterswijk, C.; de Boer, J. Spheroid culture as a tool for creating 3D complex tissues. *Trends Biotechnol.* **2013**, *31* (2), 108−115.
(12) Yang, M.; Chen, C.; Lin, P.; Huang, C.; Chen, W.; Sung, H. Novel method of forming human embryoid bodies in a polystyrene dish surface-coated with a temperature-responsive methylcellulose hydrogel. *Biomacromolecules* **2007**, *8*, 2746−2752.
(13) Sarvi, F.; Arbatan, T.; Chan, P.; Shen, W. A novel technique for the formation of embryoid bodies inside liquid marbles. *RSC Adv.* **2013**, *3*, 14501−14508.
(14) Hardelauf, H.; Frimat, J.-P.; Stewart, J. D.; Schormann, W.; Chiang, Y.-Y.; Lampen, P.; Franzke, J.; Hengstler, J. G.; Cadenas, C.; Kunz-Schughart, L. A.; West, J. Microarrays for the scalable production of metabolically relevant tumour spheroids: a tool for modulating chemosensitivity traits. *Lab Chip* **2011**, *11* (3), 419−428.
(15) (a) Jin, H.-J.; Cho, Y.-H.; Gu, J.-M.; Kim, J.; Oh, Y.-S. A multicellular spheroid formation and extraction chip using removable cell trapping barriers. *Lab Chip* **2011**, *11* (1), 115−119. (b) Yu, L.; Chen, M. C. W.; Cheung, K. C. Droplet-based microfluidic system for multicellular tumor spheroid formation and anticancer drug testing. *Lab Chip* **2010**, *10* (18), 2424−2432. (c) Kuo, C.-T.; Chiang, C.-L.; Yun-Ju Huang, R.; Lee, H.; Wo, A. M. Configurable 2D and 3D spheroid tissue cultures on bioengineered surfaces with acquisition of epithelial-mesenchymal transition characteristics. *NPG Asia Mater.* **2012**, *4*, e27.
(16) (a) Fukuda, J.; Nakazawa, K. Hepatocyte spheroid arrays inside microwells connected with microchannels. *Biomicrofluidics* **2011**, *5* (2), 022205. (b) Kim, T.; Doh, I.; Cho, Y.-H. On-chip three-dimensional tumor spheroid formation and pump-less perfusion culture using gravity-driven cell aggregation and balanced droplet dispensing. *Biomicrofluidics* **2012**, *6* (3), 034107. (c) Hsiao, A. Y.; Torisawa, Y.-s.; Tung, Y.-C.; Sud, S.; Taichman, R. S.; Pienta, K. J.; Takayama, S. Microfluidic system for formation of PC-3 prostate cancer co-culture spheroids. *Biomaterials* **2009**, *30* (16), 3020−3027. (d) Lee, K.; Kim, C.; Young Yang, J.; Lee, H.; Ahn, B.; Xu, L.; Yoon Kang, J.; Oh, K. W. Gravity-oriented microfluidic device for uniform and massive cell spheroid formation. *Biomicrofluidics* **2012**, *6* (1), 014114.
(17) (a) Alessandri, K.; Sarangi, B. R.; Gurchenkov, V. V.; Sinha, B.; Kießling, T. R.; Fetler, L.; Rico, F.; Scheuring, S.; Lamaze, C.; Simon, A.; Geraldo, S.; Vignjević, D.; Doméjean, H.; Rolland, L.; Funfak, A.; Bibette, J.; Bremond, N.; Nassoy, P. Cellular capsules as a tool for multicellular spheroid production and for investigating the mechanics of tumor progression in vitro. *Proc. Natl. Acad. Sci. U. S. A.* **2013**, *110* (37), 14843−14848. (b) Chan, H. F.; Zhang, Y.; Ho, Y.-P.; Chiu, Y.-L.; Jung, Y.; Leong, K. W., Rapid formation of multicellular spheroids in double-emulsion droplets with controllable microenvironment. *Sci. Rep.* **2013**, *3*, DOI: 10.1038/srep03462 (c) Kim, C.; Chung, S.; Kim, Y. E.; Lee, K. S.; Lee, S. H.; Oh, K. W.; Kang, J. Y. Generation of core-shell microcapsules with three-dimensional focusing device for efficient formation of cell spheroid. *Lab Chip* **2011**, *11* (2), 246−252.
(18) Vanherberghen, B.; Manneberg, O.; Christakou, A.; Frisk, T.; Ohlin, M.; Hertz, H.; Önfelt, B.; Wiklund, M. Ultrasound-controlled cell aggregation in a multi-well chip. *Lab Chip* **2010**, *10*, 2727−2732.
(19) (a) Ota, H.; Miki, N. Microfluidic experimental platform for producing size-controlled three-dimensional spheroids. *Sens. Actuators, A* **2011**, *169* (2), 266−273. (b) Kwapiszewska, K.; Michalczuk, A.; Rybka, M.; Kwapiszewski, R.; Brzózka, Z. A microfluidic-based platform for tumour spheroid culture, monitoring and drug screening. *Lab Chip* **2014**, *14*, 2096−2104.
(20) Al-Abboodi, A.; Fu, J.; Doran, P. M.; Tan, T. T. Y.; Chan, P. P. Y. Injectable 3D Hydrogel Scaffold with Tailorable Porosity Post-Implantation. *Adv. Healthcare Mater.* **2014**, *3* (5), 725−736.
(21) Yeo, L. Y.; Chang, H.-C.; Chan, P. P. Y.; Friend, J. R. Microfluidic Devices for Bioapplications. *Small* **2011**, *7* (1), 12−48.
(22) Friend, J.; Yeo, L. Y. Microscale acoustofluidics: Microfluidics driven via acoustics and ultrasonics. *Rev. Mod. Phys.* **2011**, *83* (2), 647−704.
(23) Shilton, R. J.; Yeo, L. Y.; Friend, J. R. Quantification of surface acoustic wave induced chaotic mixing-flows in microfluidic wells. *Sens. Actuators, B* **2011**, *160* (1), 1565−1572.
(24) Shilton, R.; Tan, M. K.; Yeo, L. Y.; Friend, J. R. Particle concentration and mixing in microdrops driven by focused surface acoustic waves. *J. Appl. Phys.* **2008**, *104* (1), 014910.
(25) Rogers, P. R.; Friend, J. R.; Yeo, L. Y. Exploitation of Surface Acoustic Waves to Drive Size-Dependent Microparticle Concentration Within a Droplet. *Lab Chip* **2010**, *10*, 2979−2985.
(26) Glass, N. R.; Shilton, R. J.; Chan, P. P. Y.; Friend, J. R.; Yeo, L. Y. Miniaturized Lab-on-a-Disc (miniLOAD). *Small* **2012**, *8* (12), 1881−1888.
(27) (a) Ding, X.; Li, P.; Lin, S.-C. S.; Stratton, Z. S.; Nama, N.; Guo, F.; Slotcavage, D.; Mao, X.; Shi, J.; Costanzo, F.; Huang, T. J. Surface acoustic wave microfluidics. *Lab Chip* **2013**, *13* (18), 3626−3649. (b) Yeo, L. Y.; Friend, J. R. Ultrafast microfluidics using surface acoustic waves. *Biomicrofluidics* **2009**, *3* (1), 012002. (c) Yeo, L. Y.; Friend, J. R. Surface Acoustic Wave Microfluidics. *Annu. Rev. Fluid Mech.* **2014**, *46* (1), 379−406. (d) Dung Luong, T.; Trung Nguyen, N.

DOI: 10.1021/acsbiomaterials.6b00144
ACS Biomater. Sci. Eng. 2016, 2, 1013−1022

Surface Acoustic Wave Driven Microfluidics - A Review. *Micro Nanosyst.* **2010**, *2* (3), 217−225. (e) Franke, T.; Braunmüller, S.; Schmid, L.; Wixforth, A.; Weitz, D. A. Surface acoustic wave actuated cell sorting (SAWACS). *Lab Chip* **2010**, *10*, 789−794. (f) Frommelt, T.; Kostur, M.; Wenzel-Schäfer; Talkner, P.; Hänggi, P.; Wixforth, A. Microfluidic Mixing via Acoustically Driven Chaotic Advection. *Phys. Rev. Lett.* **2008**, *100*, 034502.

(28) Li, H.; Friend, J.; Yeo, L.; Dasvarma, A.; Traianedes, K. Effect of surface acoustic waves on the viability, proliferation and differentiation of primary osteoblast-like cells. *Biomicrofluidics* **2009**, *3* (3), 034102.

(29) (a) Ding, X.; Lin, S.-C. S.; Kiraly, B.; Yue, H.; Li, S.; Chiang, I.-K.; Shi, J.; Benkovic, S.; Huang, T. On-chip manipulation of single microparticles, cells, and organisms using surface acoustic waves. *Proc. Natl. Acad. Sci. U. S. A.* **2012**, *109*, 11105−11109. (b) Guo, F.; Li, P.; French, J.; Mao, Z.; Zhao, H.; Li, S.; Nama, N.; Fick, J.; Benkovic, S.; Huang, T. Controlling cell−cell interactions using surface acoustic waves. *Proc. Natl. Acad. Sci. U. S. A.* **2015**, *112*, 43−48.

(30) (a) Li, H.; Friend, J.; Yeo, L.; Dasvarma, A.; Traianedes, K. Effect of Surface Acoustic Waves on the Viability, Proliferation and Differentiation of Primary Osteoblast-Like Cells. *Biomicrofluidics* **2009**, *3*, 034102. (b) Alhasan, L.; Qi, A.; Rezk, A. R.; Yeo, L. Y.; Chan, P. P. Y. Assessment of the potential of a high frequency acoustomicrofluidic nebulisation platform for inhaled stem cell therapy. *Integrative Biology* **2016**, *8* (1), 12−20.

(31) Holliday, D. L.; Speirs, V. Choosing the right cell line for breast cancer research. *Breast Cancer Research* **2011**, *13*, 215.

(32) (a) Monazzam, A.; Razifar, P.; Simonsson, M.; Qvarnström, F.; Josephsson, R.; Blomqvist, C.; Långström, B.; Bergström, M. Multicellular Tumour Spheroid as a model for evaluation of [^{18}F]FDG as biomarker for breast cancer treatment monitoring. *Cancer Cell Int.* **2006**, *6*, 6. (b) Howes, A. L.; Richardson, R. D.; Finlay, D.; Vuori, K. 3-Dimensional Culture Systems for Anti-Cancer Compound Profiling and High-Throughput Screening Reveal Increases in EGFR Inhibitor-Mediated Cytotoxicity Compared to Monolayer Culture Systems. *PLoS One* **2014**, *9* (9), e108283. (c) Sakamoto, R.; Rahman, M. M.; Shimomura, M.; Itoh, M.; Nakatsura, T. Time-lapse imaging assay using the BioStation CT: A sensitive drug-screening method for three-dimensional cell culture. *Cancer Science* **2015**, *106* (6), 757−765.

(33) (a) Bartosh, T. J.; Ylöstalo, J. H.; Mohammadipoor, A.; Bazhanov, N.; Coble, K.; Claypool, K.; Lee, R. H.; Choi, H.; Prockop, D. J. Aggregation of human mesenchymal stromal cells (MSCs) into 3D spheroids enhances their antiinflammatory properties. *Proc. Natl. Acad. Sci. U. S. A.* **2010**, *107* (31), 13724−13729. (b) Baraniak, P. R.; McDevitt, T. C. Scaffold-free culture of mesenchymal stem cell spheroids in suspension preserves multilineage potential. *Cell Tissue Res.* **2012**, *347* (3), 701−711. (c) Yamaguchi, Y.; Ohno, J.; Sato, A.; Kido, H.; Fukushima, T. Mesenchymal stem cell spheroids exhibit enhanced in-vitro and in-vivo osteoregenerative potential. *BMC Biotechnol.* **2014**, *14* (1), 1−10.

(34) (a) Hodgson, R.; Tan, M.; Yeo, L.; Friend, J. Transmitting high power rf acoustic radiation via fluid couplants into superstrates for microfluidics. *Appl. Phys. Lett.* **2009**, *94*, 024102. (b) Bourquin, Y.; Reboud, J.; Wilson, R.; Cooper, J. Tuneable surface acoustic waves for fluid and particle manipulations on disposable chips. *Lab Chip* **2010**, *10*, 1898−1901. (c) Wilson, R.; Reboud, J.; Bourquin, Y.; Neale, S.; Zhang, Y.; Cooper, J. Phononic crystal structures for acoustically driven microfluidic manipulations. *Lab Chip* **2011**, *11*, 323−328.

(35) Li, H.; Friend, J.; Yeo, L. Surface acoustic wave concentration of particle and bioparticle suspensions. *Biomed. Microdevices* **2007**, *9* (5), 647−656.

(36) Fischer, A. H.; Jacobson, K. A.; Rose, J.; Zeller, R. Hematoxylin and Eosin Staining of Tissue and Cell Sections. *Cold Spring Harbor Protocols* **2008**, pdb.prot4986.

(37) Yu, H.; Lim, K. P.; Xiong, S.; Tan, L. P.; Shim, W. Functional Morphometric Analysis in Cellular Behaviors: Shape and Size Matter. *Adv. Healthcare Mater.* **2013**, *2* (9), 1188−1197.

(38) Hoo, S.; Sarvi, F.; Li, W.; Chan, P.; Yue, Z. Thermoresponsive Cellulosic Hydrogels with Cell-Releasing Behavior. *ACS Appl. Mater. Interfaces* **2013**, *5*, 5592−5600.

(39) Raghavan, R. V.; Friend, J. R.; Yeo, L. Y. Particle Concentration via Acoustically Driven Microcentrifugation: MicroPIV Flow Visualization and Numerical Modelling Studies. *Microfluid. Nanofluid.* **2010**, *8*, 73−84.

(40) Lee, Y.-H.; Peng, C.-A. Nonviral Transfection of Suspension Cells in Ultrasound Standing Wave Fields. *Ultrasound in Medicine & Biology* **2007**, *33* (5), 734−742.

(41) Mueller, S.; Llewellin, E. W.; Mader, H. M. The rheology of suspensions of solid particles. *Proc. R. Soc. London, Ser. A* **2010**, *466* (2116), 1201−1228.

(42) Carlo, D. D.; Wu, L. Y.; Lee, L. P. Dynamic single cell culture array. *Lab Chip* **2006**, *6* (11), 1445−1449.

(43) McGahon, A.; Martin, S.; Bissonnette, R.; Mahboubi, A.; Shi, Y.; Mogil, R.; Nishioka, W.; Green, D. The end of the (cell) line: methods for the study of apoptosis in vitro. *Methods Cell Biol.* **1995**, *46*, 153−185.

(44) Sutherland, R. M. Cell and environment interactions in tumor microregions: the multicell spheroid model. *Science* **1988**, *240* (4849), 177−184.

(45) Lee, S.; Jeon, H.; Kim, C.; Ju, M.; Bae, H.; Park, H.; Lim, S.-C.; Han, S.; Kang, H. Homeobox gene Dlx-2 is implicated in metabolic stress-induced necrosis. *Mol. Cancer* **2011**, *10*, 113.

(46) Ma, H.-l.; Jiang, Q.; Han, S.; Wu, Y.; Tomshine, J.; Wang, D.; Gan, Y.; Zou, G.; Liang, X.-J. Multicellular Tumor Spheroids as n in Vivo Tumor Model for Three-Dimensional Imaging of Chemotherapeutic and Nano Material Cellular Penetration. *Mol. Imaging* **2012**, *11*, 487−498.

(47) Kunz-Schughart, L. A.; Kreutz, M.; Knuechel, R. Multicellular spheroids: a three-dimensional in vitro culture system to study tumour biology. *Int. J. Exp. Pathol.* **1998**, *79* (1), 1−23.

DOI: 10.1021/acsbiomaterials.6b00144
ACS Biomater. Sci. Eng. 2016, 2, 1013−1022